

Inferring learning rules from distributions of firing rates in cortical neurons

Sukbin Lim¹, Jillian L McKee¹, Luke Woloszyn², Yali Amit^{3,4}, David J Freedman¹, David L Sheinberg⁵ & Nicolas Brunel^{1,3}

Information about external stimuli is thought to be stored in cortical circuits through experience-dependent modifications of synaptic connectivity. These modifications of network connectivity should lead to changes in neuronal activity as a particular stimulus is repeatedly encountered. Here we ask what plasticity rules are consistent with the differences in the statistics of the visual response to novel and familiar stimuli in inferior temporal cortex, an area underlying visual object recognition. We introduce a method that allows one to infer the dependence of the presumptive learning rule on postsynaptic firing rate, and we show that the inferred learning rule exhibits depression for low postsynaptic rates and potentiation for high rates. The threshold separating depression from potentiation is strongly correlated with both mean and s.d. of the firing rate distribution. Finally, we show that network models implementing a rule extracted from data show stable learning dynamics and lead to sparser representations of stimuli.

Reorganization of neuronal circuits through experience-dependent synaptic modification has been postulated to be one of the basic mechanisms for learning and memory¹. This idea is supported by experimental work from different preparations that show long-term changes of synaptic strengths induced by various patterns of pre- and postsynaptic activity^{2–6}. Such activity-dependent synaptic modifications in a neural circuit would in turn lead to changes of activity of the circuit. A positive feedback between synaptic potentiation and elevated neuronal activity could lead to enhanced neuronal responses, while synaptic depression would lead to opposite changes.

While changes of synaptic strengths in strongly connected cortical circuits are difficult to identify *in vivo*, changes of single-neuron responses *in vivo* have been suggested as evidence for synaptic plasticity in cortical circuits. In particular, perturbations in input statistics or perceptual learning tasks have been shown to induce changes in neuronal responses^{7–9}. Theoretical models have been used to understand interactions between activity-dependent plasticity rules and network activity^{10,11}. Such models typically implement synaptic plasticity rules extracted from *in vitro* studies, and they provide qualitative explanations for changes of sensory representations in feedforward circuits^{12,13} and changes of sensory and memory-related activity in recurrently connected circuits^{14,15}.

One of the cortical areas where the effects of sensory experience on neuronal responses have been documented is inferior temporal cortex (ITC), an area that is critical for visual object perception and recognition^{16–18}. Two types of experiments have been used, one in which initially novel visual stimuli are shown repeatedly to a monkey¹⁹ and another in which two sets of stimuli (novel and familiar) are compared^{18,20–24}. Several effects of visual experience on ITC neuronal

activity and selectivity have been described in these studies. First, it has been shown that repeated presentations of an initially novel stimulus in a single recording session lead to a gradual decrease of visual responses to the stimulus in a substantial fraction of recorded neurons¹⁹. Second, comparisons between visual responses to novel stimuli and stimuli that have been presented over many recording sessions have demonstrated that the response to familiar stimuli is typically more selective^{18,20–23}, with higher maximum responses to familiar stimuli in putative excitatory neurons²². However, it is still unclear what type of learning rules could explain these data.

Here we introduce a procedure that allowed us to derive the synaptic plasticity rule from changes in distributions of visual responses to novel and familiar stimuli, using a cortical network model composed of excitatory and inhibitory neurons whose excitatory-to-excitatory connectivity is plastic. We applied this method to experimental data obtained in ITC neurons in monkeys performing two different tasks, a passive fixation task²² and a dimming-detection task²⁵. Finally, we showed that simulations implementing learning rules derived from data in a recurrent network model provide a good match with experimental data.

RESULTS

Changes in network response induced by synaptic plasticity

To investigate the relation between synaptic plasticity rule and changes of network activity with learning, we considered a firing rate model with a plasticity rule that modifies the strength of recurrent synapses as a function of the firing rates of pre- and postsynaptic neurons. Activities of neurons are described by their firing rates r_i , $i = 1, \dots, N$, where N denotes the number of neurons

¹Department of Neurobiology, University of Chicago, Chicago, Illinois, USA. ²Department of Neuroscience, Columbia University, New York, New York, USA. ³Department of Statistics, University of Chicago, Chicago, Illinois, USA. ⁴Department of Computer Science, University of Chicago, Chicago, Illinois, USA. ⁵Department of Neuroscience, Brown University, Providence, Rhode Island, USA. Correspondence should be addressed to N.B. (nbrunel@uchicago.edu).

Received 5 August; accepted 7 October; published online 2 November 2015; doi:10.1038/nn.4158

Figure 1 Visual response of inferior temporal cortical (ITC) neurons to novel and familiar stimuli. (a–d) Time course of mean (a,b) and maximal (c,d) visual responses of ITC excitatory (a,c) and inhibitory (b,d) neurons obtained in a passive viewing task²². Solid curves are activities averaged over all neurons for novel (red) or familiar (blue) stimuli, and shaded regions represent mean \pm s.e.m. of activities averaged over individual neurons (a–d). The gray horizontal bar represents the visual stimulation period. For more details of the experiment, see Online Methods and ref. 22.

in the network. The firing rate of neuron i depends on its inputs h_i through a static transfer function (f - I curve) Φ_i as

$$r_i = \Phi_i(h_i), \quad \text{with} \quad h_i = I_{iX} + \sum_{j=1}^N W_{ij}r_j \quad (1)$$

The input current h_i is the sum of the external input I_{iX} and the recurrent input, which is itself a sum of presynaptic firing rates r_j , weighted by the synaptic strength W_{ij} connecting neuron j to neuron i .

We investigated how the network response changes with visual experience as initially novel stimuli become familiar. Changes due to visual experience could in principle come from changes in external inputs, recurrent inputs or both. Here we assume that changes in network response are primarily due to changes in recurrent synapses. This assumption is justified by the observation that differences between responses to familiar and novel stimuli start to emerge a few tens of milliseconds after the activity onset^{21–23} (Fig. 1). We therefore assumed that the recurrent synapses are plastic, changing their strength according to $W_{ij} \rightarrow W_{ij} + \Delta W(r_i, r_j)$, where the synaptic change $\Delta W(r_i, r_j)$ depends on firing rates of both pre- and postsynaptic neurons during the presentation of the stimulus. The changes in synaptic strengths lead to changes in synaptic inputs to neurons, $h_i \rightarrow h_i + \Delta h_i$, and consequently to changes in their firing rates $r_i \rightarrow r_i + \Delta r_i$, according to

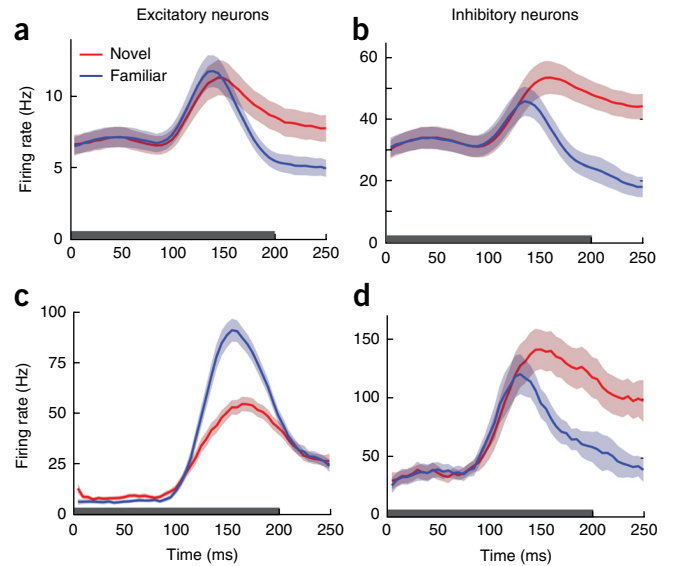
$$r_i + \Delta r_i = \Phi_i(h_i + \Delta h_i) \\ \text{with} \quad h_i + \Delta h_i = I_{iX} + \sum_{j=1}^N (W_{ij} + \Delta W(r_i, r_j))(r_j + \Delta r_j) \quad (2)$$

Note that since synaptic plasticity occurs only in recurrent connections, changes of recurrent synaptic inputs are the only source of input changes, so that henceforth input changes refer to changes of recurrent inputs only, unless specified otherwise.

When $\Delta W(r_i, r_j)$ and Δr_j are small compared to W_{ij} and r_j , respectively, $\sum_{j=1}^N \Delta W(r_i, r_j)\Delta r_j$ can be neglected in comparing equation (1) and equation (2), and the changes in inputs become approximately

$$\Delta h_i \approx \sum_{j=1}^N \Delta W(r_i, r_j)r_j + \sum_{j=1}^N W_{ij}\Delta r_j \quad (3)$$

Equation (3) shows two different contributions of $\Delta W(r_i, r_j)$ to input changes Δh_i : the first term on the right side represents a direct influence of changes of synaptic strengths projecting onto a postsynaptic neuron on the inputs to that neuron, and the second term represents an indirect influence through changes of presynaptic firing rates that reflect changes of synaptic strengths in the whole network. On the basis of the above equations, we can calculate changes in firing rates Δr_j when the transfer functions Φ_i and the synaptic plasticity rule $\Delta W(r_i, r_j)$ are known (see the analytic



expression of firing rates and its application to an example learning rule in **Supplementary Math Note**, section 1).

Inferring learning rules from firing rate distributions

We now ask the inverse question: can we infer the synaptic plasticity rule from the changes of network responses with learning? To perform this inference, we make the assumption that the learning rule is a separable function of pre- and postsynaptic rates, $\Delta W(r_i, r_j) = f_{\text{post}}(r_i)f_{\text{pre}}(r_j)$. Then the dependence of the learning rule on postsynaptic firing rates $f_{\text{post}}(r_i)$ can be obtained from equation (3) as

$$\Delta h_i \approx \sum_{j=1}^N \Delta W(r_i, r_j)r_j + \sum_{j=1}^N W_{ij}\Delta r_j = f_{\text{post}}(r_i) \sum_{j=1}^N f_{\text{pre}}(r_j)r_j + \sum_{j=1}^N W_{ij}\Delta r_j \\ \Rightarrow f_{\text{post}}(r_i) \approx \left(\Delta h_i - \sum_{j=1}^N W_{ij}\Delta r_j \right) / \sum_{j=1}^N f_{\text{pre}}(r_j)r_j \quad (4)$$

These equations allow us to estimate the function $f_{\text{post}}(r_i)$, characterizing how synaptic plasticity depends on the postsynaptic firing rate, from the distributions of responses to novel and familiar stimuli, using a few more assumptions that we detail below. The method is illustrated in **Figure 2** using the distributions of firing rates of a single ITC neuron, computed from the response of the neuron to 125 novel stimuli and 125 familiar stimuli²² (Fig. 2a; see Online Methods). These distributions are similar to log-normal distributions, as has been noted previously in other areas^{26–28}. The distribution of responses to familiar stimuli is shifted to the left of the distribution of responses to novel stimuli, indicating that, on average, familiar stimuli elicit lower rates than novel stimuli, but the tail of the distribution of familiar responses extends further to the right than the distribution of novel responses.

From these empirical distributions, the inference of synaptic changes was done in four steps (**Supplementary Fig. 1**). First, we deduced the transfer function Φ from the distribution of responses for novel stimuli, under two assumptions: (i) the transfer function is monotonically increasing; that is, higher input currents lead to higher output firing rates, consistent with both *in vivo* and *in vitro* electrophysiological data^{29,30}, and (ii) input currents for novel stimuli follow a normal distribution. This assumption is based on the central limit theorem: since cortical neurons receive a very large number

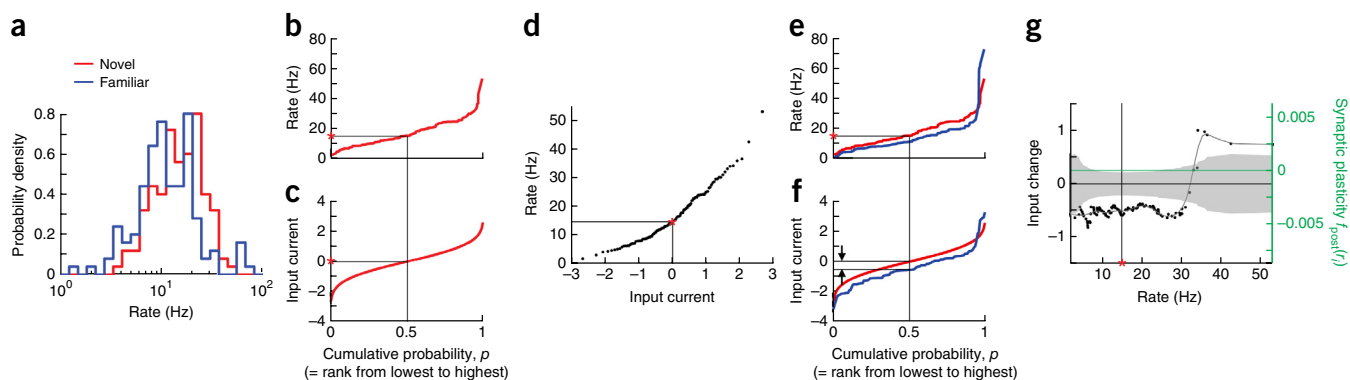


Figure 2 Inferring learning rules from distributions of firing rates. **(a)** Distributions of firing rates of a single ITC neuron in response to novel (red) and familiar (blue) stimuli. **(b–d)** Deriving a static transfer function Φ from the distribution of visual responses for novel stimuli. **(b,c)** Inverse cumulative distribution functions of firing rates **(b)** and input current **(c)** to novel stimuli, obtained by ordering them according to their rank. Input currents were assumed to follow Gaussian statistics and were normalized by their means and s.d., yielding mean and variance 0 and 1, respectively. Red asterisks are the median firing rate and input current ($p = 0.5$). **(d)** Input current–output firing rate transfer function Φ . The red asterisk in **d** shows the firing rate and input current for $p = 0.5$ (corresponding to red asterisks in **b** and **c**). **(e–g)** Inferring input changes and learning rules. **(e,f)** Inverse cumulative distribution functions of firing rates **(e)** and input currents **(f)** for novel (red) and familiar (blue) stimuli. **(g)** Input changes (left axis) and dependence of learning rule on the postsynaptic firing rate (right axis). The black vertical line and red asterisk indicate the median firing rate for novel stimuli and the corresponding input change. The dependence of the synaptic plasticity rule on the postsynaptic firing rate is obtained from input changes through a constant offset and rescaling. The constant offset and scaling factor are chosen to be 0.25 and 200, respectively, for illustration. The curve is a smoothed input change curve and the gray area represents a 95% confidence region (see Online Methods).

of inputs, which, in the case of novel stimuli, can be assumed to be weakly correlated, the distribution of total synaptic inputs is likely to follow approximately Gaussian statistics. Under these two assumptions, the transfer function (f - I curve) is obtained from the empirical distribution of rates for novel stimuli and the assumed Gaussian distribution of input currents as follows. Input currents and rates are ordered according to rank (**Fig. 2b,c**). Because the f - I curve is assumed to be monotonically increasing, ranks are preserved and the firing rate dependence on the input current is obtained by matching corresponding ranks (**Fig. 2d**). The obtained f - I curve resembles qualitatively the experimentally measured f - I curves of pyramidal cells in the presence of noise^{29,30}.

Input currents for familiar stimuli were obtained from firing rates by applying the inverse of the derived transfer function, assuming that the transfer function remains unchanged with learning (**Fig. 2e,f**). We then compare the distributions of input currents for novel and familiar stimuli and extract how input changes with learning as a function of the response to novel stimuli. Since we do not have recordings of the neuron's response to the very same stimulus as it transitions from novel to familiar, to perform this step, we need one last assumption: given a set of initially novel stimuli leading to a set of responses, learning these stimuli does not change the rank of the corresponding responses. This allows us to compare responses to two different stimuli, one novel and one familiar, that have the same rank. For example, for a novel stimulus that elicits a median response (about 15 Hz in the example in **Fig. 2e**), we expect learning to decrease the rate to the median response to familiar stimuli (about 10 Hz in **Fig. 2e**). Under the rank preservation assumption, the input changes are computed by comparing input currents for novel and familiar stimuli at the same rank (**Fig. 2e,f**). Input changes are plotted as a function of postsynaptic firing rate before learning; that is, Δh as a function of r_{post} (see equation (3); **Fig. 2g**). We remark that the rank preservation assumption minimizes $\sum (\Delta r_i)^2$ among all possible sets of Δr_i (**Supplementary Math Note**, section 2). Thus, it is consistent with the assumption of small changes of synaptic strengths and firing rates, ΔW_{ij} and Δr_j , in our derivation of learning rules in equations (3) and (4).

Finally, from the function $\Delta h(r_i)$, we obtained a synaptic plasticity rule whose dependence on the postsynaptic firing rate $f_{\text{post}}(r_i)$ has a similar form to that of the input changes (**Fig. 2g**). According to equation (4), $f_{\text{post}}(r_i)$ can be obtained by subtracting input changes due to changes of firing rates $\sum_j W_{ij} \Delta r_j$ from total input changes $\Delta h(r_i)$ and normalizing it with a term containing the dependence of the learning rule on presynaptic firing rates, $\sum_j f_{\text{pre}}(r_j) r_j$. Note that $\sum_j f_{\text{pre}}(r_j) r_j$ is constant for all neurons, and we assume that $\sum_j W_{ij} \Delta r_j$ is approximately independent of r_i . Thus, the dependence of the learning rule on postsynaptic firing rate $f_{\text{post}}(r_i)$ can be obtained from input changes by subtracting a constant offset and rescaling its magnitude (**Fig. 2g**).

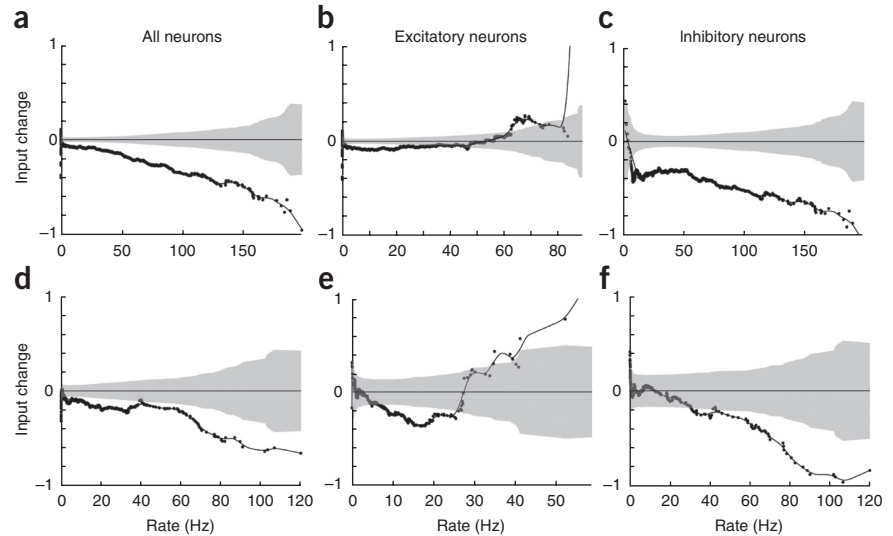
The derived learning rules depend on the assumptions we made on input statistics, properties of the transfer function and properties of the learning rules. However, our results remain qualitatively unchanged if these assumptions are relaxed. Transfer functions and learning rules derived assuming non-Gaussian statistics of input currents for novel stimuli (**Supplementary Fig. 2**) or starting with the input statistics for familiar stimuli (**Supplementary Fig. 3**) are qualitatively similar to the original ones. Also, we note that even if the assumption of the rank preservation of a stimulus is relaxed with the addition of noise to input currents, it is found that input changes computed under the relaxed assumption show similar dependence on postsynaptic firing rates (**Supplementary Fig. 4**).

Inferred ITC learning rules

Using the method illustrated above, we investigated the effect of visual experience in inferior temporal cortex (ITC) using neurophysiological data obtained from two different laboratories in monkeys performing two different tasks, one a passive viewing task²² and the other a dimming-detection task²⁵ (see Online Methods). In both cases, we obtained the distributions of neural activities to novel or familiar stimuli by taking firing rates of neurons averaged during the stimulus presentation period.

Despite the difference in tasks and the number of stimuli used to measure activities in each neuron, we found similar input changes with learning in the two data sets, whose shape depended on cell

Figure 3 Effect of visual experience in ITC neurons and their dependence on different cell types. (a–c) Input changes obtained from visual responses of ITC neurons in monkeys performing a passive viewing task. The input currents were obtained from the distributions of firing rates for novel and familiar stimuli that were averaged over all recorded neurons ($n = 88$). Only negative changes are observed with learning (a; see Online Methods for smoothing procedure). When neurons were grouped as putative excitatory ($n = 73$) and inhibitory ($n = 15$) neurons, excitatory neurons showed negative changes for low postsynaptic firing rate and positive changes for high rate (b), while inhibitory neurons showed only negative changes (c). (d–f) Input changes obtained in monkeys performing a dimming-detection task. As in the passive viewing task (a–c), the input changes obtained from all recorded neurons (d, $n = 221$) and from putative inhibitory neurons (f) showed only decrease, while putative excitatory neurons showed both negative and positive changes (e). Note that putative neuronal classes were determined from the spike widths. To minimize potential misclassifications in the dimming-detection task, we set well-separated thresholds for putative excitatory and inhibitory neurons, leading to 41 and 27 neurons classified as excitatory and inhibitory neurons, respectively (see Online Methods).



type—putative excitatory or putative inhibitory (Fig. 3). When the distributions of firing rates for novel and familiar stimuli were averaged over all recorded neurons, input currents showed negative changes with learning for all postsynaptic firing rates. These changes were below the 95% confidence region obtained from computing this curve using random samples from the novel distribution instead of the familiar distribution (Fig. 3a,d; see Online Methods). This is consistent with experimental observations that average firing rates decrease with familiarity^{21–23}. Next we applied the analysis separately to putative excitatory and inhibitory cells, defined by the width of action potential waveforms (see Online Methods). Excitatory neurons showed negative changes when the postsynaptic firing rate was low, but positive changes when it was high (Fig. 3b,e). Such positive input changes in a high firing rate regime are consistent with the increase of maximal responses of excitatory neurons with learning that have been observed experimentally^{16,18,20,22}. Inhibitory neurons showed negative input changes at all firing rates (Fig. 3c,f). Note that averaging over both groups of neurons completely masks the enhancement of input currents in excitatory neurons at high rates (Fig. 3a,d) because of the stronger negative input changes in inhibitory neurons (Fig. 3c,f).

In the experimental data obtained during the passive viewing task, we further analyzed the learning effects on input currents in individual neurons (Fig. 4). To compare input changes in neurons with a different range of firing rates, we normalized firing rates of postsynaptic neurons by subtracting their mean and dividing by the s.d. of firing rates to different stimuli (Fig. 4a,b). In excitatory neurons, we found diverse patterns of input changes that can be classified into three categories (Fig. 4a): neurons showing only negative changes, neurons showing negative changes for low firing rates and positive changes for high firing rates, and neurons showing only positive changes. Despite diverse patterns, the input changes in the excitatory neurons were increasing as normalized firing rates increase, except for a few neurons showing only negative changes and having high mean firing rates (Fig. 4a). These diverse patterns of input changes may result from a different constant offset in input changes in each neuron (the first term on the right side of equation (3)), rather than different forms of rules governing synaptic plasticity onto

different neurons. Averaging the input change curves of excitatory neurons showing both negative and positive changes (Fig. 4a) led to depression for low firing rates and potentiation for high firing rates, consistent with previous *in vitro* experiments^{6,31} (Fig. 4c). Note also that the transfer functions of different neurons with normalized firing rates were very similar to each other (Supplementary Fig. 5).

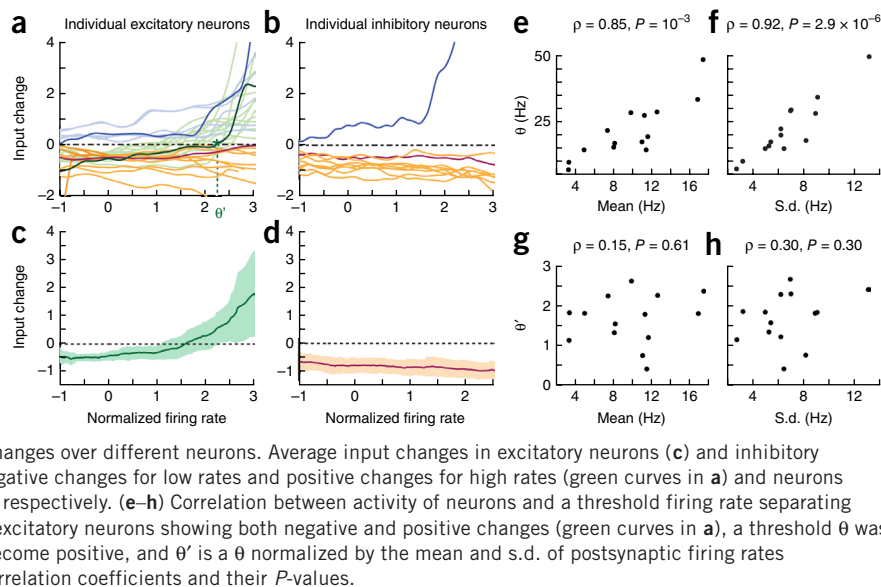
For neurons showing both negative and positive changes, we defined a threshold θ as the postsynaptic firing rate where input changes become positive. We denote the normalized threshold, obtained by subtracting the mean rate and dividing by the s.d. of the rate, as θ' (Fig. 4a). We found that the threshold θ was strongly correlated with both mean and s.d. of postsynaptic firing rates (Fig. 4e,f), but such correlation disappeared for the normalized threshold θ' (Fig. 4g,h). This suggests that a threshold between depression and potentiation in the synaptic plasticity rule is dependent on activity of neurons, which is reminiscent of the Bienenstock-Cooper-Munro learning rule¹². The threshold observed in ITC neurons is around 1.5 s.d. above the mean firing rate (Fig. 4c), consistent with a scenario in which a large majority of stimuli lead to depression, while a small minority (the ones with the strongest responses) lead to potentiation.

Changes of input currents derived from the statistics of individual inhibitory neurons were similar to those from the statistics of their population average: except for one neuron showing positive changes, inhibitory neurons showed negative input changes (Fig. 4b) that depended only weakly on firing rates (Fig. 4d). Firing rate-independent negative changes can be explained by a decrease in average firing rates of the excitatory subnetwork that would cause decrease in inputs from excitatory to inhibitory neurons (see equation (3)), in the absence of any plasticity mechanism in inhibitory neurons. A similar shape of negative input changes was observed in a few putative excitatory neurons (Fig. 4a). These neurons have a similar dynamic range of activity to inhibitory neurons with high mean firing rates and may be inhibitory neurons with broad spike widths.

Simulations and comparison to the data

We next addressed whether a network model with a learning rule inferred from data can maintain stable learning dynamics as it is subjected to multiple novel stimuli and whether the changes of activity

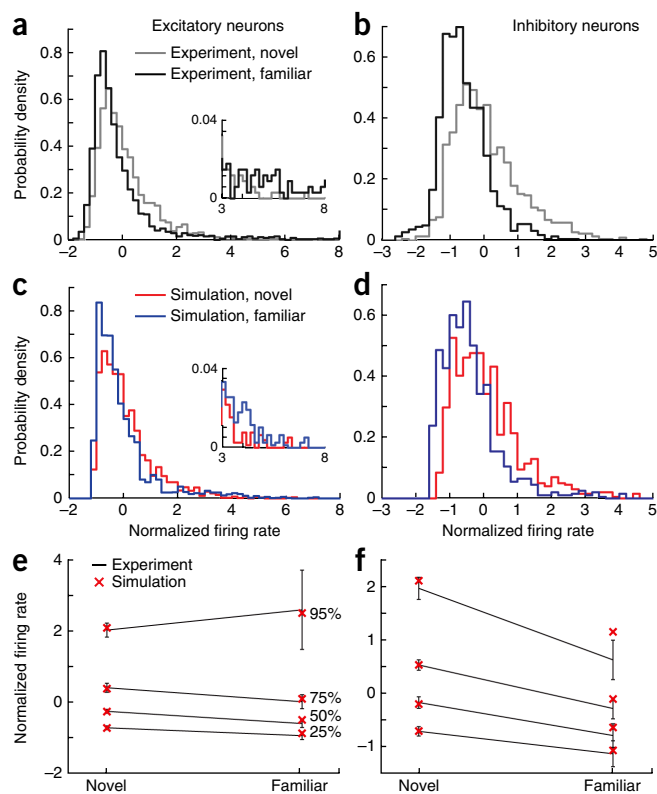
Figure 4 Effect of visual experience in individual ITC neurons and regulation of learning rules. (**a,b**) Input changes obtained from visual responses of individual excitatory (**a**, $n = 30$) and inhibitory (**b**, $n = 10$) neurons. Firing rates of postsynaptic neurons to novel stimuli were normalized by their mean and s.d., and input changes were smoothed (see Online Methods). Neurons were classified into three categories: those showing only negative changes (orange; 10 excitatory and 9 inhibitory neurons), only positive changes (blue; 6 excitatory neurons and 1 inhibitory), and both negative and positive changes (green; 14 excitatory neurons). Dark curves are example neurons in each class. (**c,d**) Average input changes in excitatory neurons (**c**) and inhibitory neurons (**d**), with shaded areas representing 1.96 s.d. of input changes over different neurons. Average input changes in excitatory neurons (**c**) and inhibitory neurons (**d**) were obtained from neurons showing negative changes for low rates and positive changes for high rates (green curves in **a**) and neurons showing only negative changes (orange curves in **b**), respectively. (**e-h**) Correlation between activity of neurons and a threshold firing rate separating potentiation from depression in input currents. For excitatory neurons showing both negative and positive changes (green curves in **a**), a threshold θ was defined as the firing rate for which input changes become positive, and θ' is a θ normalized by the mean and s.d. of postsynaptic firing rates (green asterisk in **a**). ρ and P in each plot are the correlation coefficients and their P -values.



patterns with learning observed in the experiment can be reproduced. Simulated networks were composed of excitatory (E) and inhibitory (I) neurons and were initially fully connected. All neurons of a given type (E or I) had the same input-output transfer functions. Cells of the same type had the same distributions of firing rates, which were derived from data (see Online Methods). Synaptic plasticity was implemented in excitatory-to-excitatory (E-to-E) connections only, while all connections involving inhibition were fixed. The motivation for restricting plasticity to E-to-E connections is that, as we will see below, this is the simplest model that was able to reproduce the data (see also **Supplementary Math Note**, section 3). All E-to-E synapses had the same firing rate-dependent learning rule, whose postsynaptic dependence was derived from data, taking into account excitatory neurons showing depression at low rates and potentiation at high rates (**Fig. 4c**). For simplicity, we took the dependence on the presynaptic rates f_{pre} to be linear (see below). We also added bounds on synaptic strengths. Note that in simulations, the synaptic strengths were updated only once per stimulus. This single update of synaptic strengths per stimulus effectively captures changes of synaptic strengths that occur gradually in time through multiple presentations until the steady state of learning is reached. Synapses from or onto inhibitory neurons were assumed to be uniform with fixed strengths.

Figure 5 Comparison between simulated and experimental data. (**a,b**) Distributions of normalized firing rates of excitatory (**a**) and inhibitory (**b**) neurons for novel (gray) and familiar (black) stimuli, obtained from experiment. The distributions were obtained from the activities of individual neurons showing characteristic input changes in each cell type (green curves in **Fig. 4a** for excitatory neurons and orange curves in **Fig. 4b** for inhibitory neurons). Firing rates for novel stimuli were normalized by the mean and s.d. for each individual neuron and distributions of normalized firing rates were averaged over neurons in each cell type (gray). The distributions for familiar stimuli (black) were obtained similarly, except that firing rates were normalized with the mean and s.d. of firing rates to novel stimuli to examine changes with learning. (**c,d**) Distributions of normalized firing rates for novel (red) and familiar (blue) stimuli, obtained from the simulation. As in the experimental data, the firing rates were normalized with mean and s.d. of firing rates for novel stimuli. (**e,f**) Changes of 25th, 50th, 75th and 95th percentiles of normalized firing rates in the data (black) and in the simulation (red cross) for excitatory (**e**) and inhibitory (**f**) neurons. In the data, we averaged percentiles obtained in individual neurons, and error bars are the s.d. of normalized firing rates over different neurons.

We initialized the excitatory connections by presenting a large number of uncorrelated activity patterns sampled from the distributions of firing rates to novel stimuli until a stable state was reached, and investigated learning dynamics at this stable state. Note that the input changes in the data showed depression for most of the postsynaptic firing rates. When we assumed that the dependence of the learning rule on the presynaptic firing rates is $f_{post}(r_j) = r_j$, from equation (4), the total sum of synaptic weights $\sum_{i,j} f_{post}(r_j) f_{pre}(r_j)$ decreased with learning. Thus, synaptic weights were stabilized after learning multiple novel stimuli without encountering instabilities that are typical of Hebbian plasticity rules^{32,33}. However, such a learning rule led to very low mean weights, since excitatory synaptic weights cannot



be negative (**Supplementary Fig. 6**). As a consequence, the effects of learning one particular stimulus on responses were much smaller than the experimentally observed ones. To prevent this, we introduced a constraint under which the total sum of synaptic strengths onto the postsynaptic neuron is preserved^{34,35} (see Online Methods). This constraint is equivalent to $f_{\text{pre}}(r_j) = r_j - \text{mean}(r)$, where $\text{mean}(r)$ is the population average of firing rates of presynaptic neurons. Such a constraint keeps $f_{\text{post}}(r_i)$ unchanged (see Online Methods and **Supplementary Math Note**, section 4).

After the initialization stage in which many patterns were presented to the network, we compared the responses of all neurons in the network to a given stimulus before and after learning. Since the network is homogenous and since novel firing rates for stimuli in the simulated network are sampled independently from the empirical distribution of novel firing rates, this can serve as a surrogate for comparing activities measured in a single neuron in response to multiple stimuli. Activity patterns before learning (**Fig. 5c,d**) were sampled from the distribution of firing rates to novel stimuli obtained from experiment (**Fig. 5a,b**). The distributions of the firing rates after learning (**Fig. 5c,d**) were obtained from simulating network dynamics with updated excitatory synaptic weights. They were similar to those from the experimental data (**Fig. 5a,b**). Average responses were reduced for both excitatory and inhibitory neurons, while a small fraction of excitatory neurons with high firing rates showed an increase (**Fig. 5c,d**). Consistently, most percentiles of the firing rate distribution decreased with learning in excitatory and inhibitory neurons (**Fig. 5e,f**), except for firing rates of excitatory neurons at high percentiles (for example, in **Fig. 5e**, the 95th percentile). These changes led to increased selectivity and increased sparseness for learned stimuli, as observed in the experimental data^{21,22}.

Because synapses onto inhibitory neurons were not plastic, changes of firing rates in inhibitory neurons reflected changes of the average firing rate of excitatory neurons. A decrease in average firing rate of excitatory neurons led to a decrease in rates for all stimuli. Hence, despite its simplicity, network simulations implementing the learning rule show stable learning dynamics and reproduce quantitatively the main features observed in the data, including the decrease of average activities in both excitatory and inhibitory neurons and the increase of selectivity in excitatory neurons.

DISCUSSION

We have introduced a method to derive input changes and learning rules from changes of firing rates in cortical neurons. In a cortical network model in which the learning rules are separable functions of pre- and postsynaptic rates, the inferred transfer functions were consistent with *in vivo* and *in vitro* electrophysiological data^{29,30} and the dependence of the excitatory synaptic plasticity rule on postsynaptic firing rate was consistent with *in vitro* synaptic plasticity data^{6,31}. Application of this method to experimental data from ITC neurons revealed several features of the inferred learning rules. First, the inferred learning rule in recurrent excitatory connections exhibits depression for low postsynaptic firing rates and potentiation for high rates, with a dominant effect of depression on average. Such a depression-dominated learning rule leads to the decrease of average firing rates observed in the data, which cannot be captured by previously suggested Hebbian learning rules^{36,37}. Second, the threshold separating depression from potentiation is strongly correlated with the mean and s.d. of postsynaptic firing rates, which suggests a regulation of learning rules depending on neuronal activity. Third, experimentally observed changes in inhibitory firing patterns can be induced by changes of excitatory firing patterns without synaptic changes onto

inhibitory neurons, although the data do not rule out such changes. Finally, implementation of the inferred learning rule in a recurrent network model shows stable learning dynamics and provides a good match to the data.

One of the key features of the inferred learning rule is a strong correlation between the threshold separating depression and potentiation and neural activity. This is reminiscent of the Bienenstock-Cooper-Munro learning rule, wherein the threshold separating depression and potentiation is a dynamic function of the postsynaptic firing rate, leading to stabilization of learning^{12,38}. However, it has been noted that the time scale for the sliding threshold needs to be sufficiently fast to avoid such instabilities^{32,33}. Our data do not allow us to investigate a possible dynamic evolution of the threshold and its contribution to stable learning, since they give us only a snapshot in the life of neurons in ITC. In addition to its role in stabilizing learning dynamics, such a regularization of the plasticity rule may contribute to enhancing selectivity to stimuli in heterogeneous populations: given that neurons have different ranges of firing rates, an adjustment of threshold depending on neuronal activity enables potentiation and depression to occur in all neurons, leading to an expansion of the range of population responses and an enhancement of selectivity with learning.

Our work provides a method to infer synaptic plasticity rules from responses to two large sets of stimuli, one novel, the other familiar. It could also be applied to an experiment that traces responses to initially novel stimuli as the stimuli became familiar. Such an experiment would in addition reveal the speed of learning, potentially provide information on an eventual dynamic evolution of the threshold separating depression and potentiation, and test the rank preservation assumption. Similar experiments have been performed previously¹⁹, but responses to a sufficiently large number of stimuli would need to be measured to access the potentiation region of the input-change versus firing-rate curve. We predict that, in such an experiment, the stimuli that elicit initially the highest firing rates would see an increase in firing rates as they are presented repeatedly, provided that a sufficiently large number of stimuli is used²².

While our model shows that synaptic plasticity in recurrent excitatory-to-excitatory connections in ITC neurons alone can explain changes of activity patterns in both excitatory and inhibitory neurons with learning, it does not rule out synaptic plasticity in other synaptic connections of ITC neurons or in other brain regions. Previous modeling work^{14,39} implemented synaptic plasticity in recurrent circuits to explain effects of visual learning on delay activity during a memory task⁴⁰. Other models have proposed learning at feedforward connections^{41,42} or combined learning at feedforward and recurrent connections¹⁵ to account qualitatively for the effect of familiarity on visual responses. None of these studies, to our knowledge, have quantitatively compared distributions of visual responses for novel and familiar stimuli, as we have done in our study. Also, note that our method could be generalized to feedforward or feedback circuits that have been suggested to be critical for object recognition^{43–45} if the activities of input and output layers are given before and after learning. To disentangle learning occurring at multiple synaptic sites or in different areas, one could potentially use the different onset times of these synaptic inputs. For example, the effect of plasticity in feedforward connections would emerge immediately at activity onset, while plasticity in the recurrent circuits would emerge with a delay corresponding to the time scales of intrinsic or synaptic time constants (**Supplementary Fig. 7**). Also, top-down signals can be affected by learning, and the effects of those would emerge with a longer latency of around 100 ms after activity onset⁴⁶.

We explored extensions of the basic rule with a few schemes of synaptic weight normalization³⁴, and more general forms of learning rules incorporating *in vitro* experiments⁶ and previous modeling work^{47–50} need to be explored. Nevertheless, our method to infer learning rules from neuronal response distributions can provide a bridge between *in vitro* studies of synaptic plasticity rules and *in vivo* data obtained in behaving animals, where synaptic changes are very difficult to measure directly, and could be applicable to other cortical circuits to further our understanding of the interactions between circuit dynamics and synaptic plasticity rules.

METHODS

Methods and any associated references are available in the [online version of the paper](#).

Note: Any Supplementary Information and Source Data files are available in the [online version of the paper](#).

ACKNOWLEDGMENTS

We thank S. Dieudonné and D. Higgins for discussions and Y. Aljadeff, K. Burbank, and M. de Pittà for feedback on the manuscript. D.L.S. has been supported by grants from the National Science Foundation (SBE-0542013) and the US National Institutes of Health (R01EY14681). D.J.F. has been supported by a NSF CAREER award, a McKnight Scholar award and the Alfred P. Sloan Foundation. J.L.M. is a recipient of a Natural Sciences and Engineering Research Council of Canada (NSERC) fellowship.

AUTHOR CONTRIBUTIONS

S.L., Y.A. and N.B. designed the research. S.L. analyzed the data, performed network simulations and prepared the figures. J.L.M., L.W., D.J.F. and D.L.S. contributed the electrophysiological data. S.L. and N.B. wrote the manuscript, with contributions from all authors.

COMPETING FINANCIAL INTERESTS

The authors declare no competing financial interests.

Reprints and permissions information is available online at <http://www.nature.com/reprints/index.html>.

- Hebb, D.O. *The Organization of Behavior* (Wiley, 1949).
- Bi, G.Q. & Poo, M.M. Synaptic modifications in cultured hippocampal neurons: dependence on spike timing, synaptic strength, and postsynaptic cell type. *J. Neurosci.* **18**, 10464–10472 (1998).
- Bliss, T.V. & Lomo, T. Long-lasting potentiation of synaptic transmission in the dentate area of the anaesthetized rabbit following stimulation of the perforant path. *J. Physiol. (Lond.)* **232**, 331–356 (1973).
- Dudek, S.M. & Bear, M.F. Homosynaptic long-term depression in area CA1 of hippocampus and effects of N-methyl-D-aspartate receptor blockade. *Proc. Natl. Acad. Sci. USA* **89**, 4363–4367 (1992).
- Markram, H., Lubke, J., Frotscher, M. & Sakmann, B. Regulation of synaptic efficacy by coincidence of postsynaptic APs and EPSPs. *Science* **275**, 213–215 (1997).
- Sjöström, P.J., Turrigiano, G.G. & Nelson, S.B. Rate, timing, and cooperativity jointly determine cortical synaptic plasticity. *Neuron* **32**, 1149–1164 (2001).
- Dan, Y. & Poo, M.M. Spike timing-dependent plasticity: from synapse to perception. *Physiol. Rev.* **86**, 1033–1048 (2006).
- Feldman, D.E. Synaptic mechanisms for plasticity in neocortex. *Annu. Rev. Neurosci.* **32**, 33–55 (2009).
- Fox, K. & Wong, R.O. A comparison of experience-dependent plasticity in the visual and somatosensory systems. *Neuron* **48**, 465–477 (2005).
- Dayan, P. & Abbott, L.F. *Theoretical Neuroscience: Computational and Mathematical Modeling of Neural Systems* (MIT Press, 2005).
- Gerstner, W. & Kistler, W.M. *Spiking Neuron Models: Single Neurons, Populations, Plasticity* (Cambridge Univ. Press, 2002).
- Bienenstock, E.L., Cooper, L.N. & Munro, P.W. Theory for the development of neuron selectivity: orientation specificity and binocular interaction in visual cortex. *J. Neurosci.* **2**, 32–48 (1982).
- Song, S., Miller, K.D. & Abbott, L.F. Competitive Hebbian learning through spike-timing-dependent synaptic plasticity. *Nat. Neurosci.* **3**, 919–926 (2000).
- Amit, D.J. & Brunel, N. Model of global spontaneous activity and local structured activity during delay periods in the cerebral cortex. *Cereb. Cortex* **7**, 237–252 (1997).
- Sohal, V.S. & Hasselmo, M.E. A model for experience-dependent changes in the responses of inferotemporal neurons. *Network* **11**, 169–190 (2000).
- Miyashita, Y. Inferior temporal cortex: where visual perception meets memory. *Annu. Rev. Neurosci.* **16**, 245–263 (1993).
- Tanaka, K. Inferotemporal cortex and object vision. *Annu. Rev. Neurosci.* **19**, 109–139 (1996).
- Kobatake, E., Wang, G. & Tanaka, K. Effects of shape-discrimination training on the selectivity of inferotemporal cells in adult monkeys. *J. Neurophysiol.* **80**, 324–330 (1998).
- Li, L., Miller, E.K. & Desimone, R. The representation of stimulus familiarity in anterior inferior temporal cortex. *J. Neurophysiol.* **69**, 1918–1929 (1993).
- Logothetis, N.K., Pauls, J. & Poggio, T. Shape representation in the inferior temporal cortex of monkeys. *Curr. Biol.* **5**, 552–563 (1995).
- Freedman, D.J., Riesenhuber, M., Poggio, T. & Miller, E.K. Experience-dependent sharpening of visual shape selectivity in inferior temporal cortex. *Cereb. Cortex* **16**, 1631–1644 (2006).
- Woloszyn, L. & Sheinberg, D.L. Effects of long-term visual experience on responses of distinct classes of single units in inferior temporal cortex. *Neuron* **74**, 193–205 (2012).
- Meyer, T., Walker, C., Cho, R.Y. & Olson, C.R. Image familiarization sharpens response dynamics of neurons in inferotemporal cortex. *Nat. Neurosci.* **17**, 1388–1394 (2014).
- Op de Beeck, H.P., Wagemans, J. & Vogels, R. Effects of perceptual learning in visual backward masking on the responses of macaque inferior temporal neurons. *Neuroscience* **145**, 775–789 (2007).
- McKee, J.L., Thomas, S.L. & Freedman, D.J. *Soc. Neurosci. Abstr.* 65.16/HH18 (2013).
- Buzsáki, G. & Mizuseki, K. The log-dynamic brain: how skewed distributions affect network operations. *Nat. Rev. Neurosci.* **15**, 264–278 (2014).
- Hromádka, T., Deweese, M.R. & Zador, A.M. Sparse representation of sounds in the unanesthetized auditory cortex. *PLoS Biol.* **6**, e16 (2008).
- Roxin, A., Brunel, N., Hansel, D., Mongillo, G. & van Vreeswijk, C. On the distribution of firing rates in networks of cortical neurons. *J. Neurosci.* **31**, 16217–16226 (2011).
- Anderson, J.S., Lampl, I., Gillespie, D.C. & Ferster, D. The contribution of noise to contrast invariance of orientation tuning in cat visual cortex. *Science* **290**, 1968–1972 (2000).
- Rauch, A., La Camera, G., Luscher, H.R., Senn, W. & Fusi, S. Neocortical pyramidal cells respond as integrate-and-fire neurons to *in vivo*-like input currents. *J. Neurophysiol.* **90**, 1598–1612 (2003).
- Kirkwood, A., Rioult, M.C. & Bear, M.F. Experience-dependent modification of synaptic plasticity in visual cortex. *Nature* **381**, 526–528 (1996).
- Toyoizumi, T., Kaneko, M., Stryker, M.P. & Miller, K.D. Modeling the dynamic interaction of Hebbian and homeostatic plasticity. *Neuron* **84**, 497–510 (2014).
- Zenke, F., Hennequin, G. & Gerstner, W. Synaptic plasticity in neural networks needs homeostasis with a fast rate detector. *PLoS Comput. Biol.* **9**, e1003330 (2013).
- Miller, K.D. & MacKay, D.J.C. The role of constraints in Hebbian learning. *Neural Comput.* **6**, 100–126 (1994).
- Bourne, J.N. & Harris, K.M. Coordination of size and number of excitatory and inhibitory synapses results in a balanced structural plasticity along mature hippocampal CA1 dendrites during LTP. *Hippocampus* **21**, 354–373 (2011).
- Amit, D.J. & Fusi, S. Learning in neural networks with material synapses. *Neural Comput.* **6**, 957–982 (1994).
- Sejnowski, T.J. Storing covariance with nonlinearly interacting neurons. *J. Math. Biol.* **4**, 303–321 (1977).
- Cooper, L.N., Intrator, N., Blais, B.S. & Shouval, H.Z. *Theory of Cortical Plasticity* (World Scientific, 2004).
- Brunel, N. Hebbian learning of context in recurrent neural networks. *Neural Comput.* **8**, 1677–1710 (1996).
- Miyashita, Y. Neuronal correlate of visual associative long-term memory in the primate temporal cortex. *Nature* **335**, 817–820 (1988).
- Bogacz, R. & Brown, M.W. Comparison of computational models of familiarity discrimination in the perirhinal cortex. *Hippocampus* **13**, 494–524 (2003).
- Norman, K.A. & O'Reilly, R.C. Modeling hippocampal and neocortical contributions to recognition memory: a complementary-learning-systems approach. *Psychol. Rev.* **110**, 611–646 (2003).
- Riesenhuber, M. & Poggio, T. Hierarchical models of object recognition in cortex. *Nat. Neurosci.* **2**, 1019–1025 (1999).
- Yamins, D.L. *et al.* Performance-optimized hierarchical models predict neural responses in higher visual cortex. *Proc. Natl. Acad. Sci. USA* **111**, 8619–8624 (2014).
- DiCarlo, J.J., Zoccolan, D. & Rust, N.C. How does the brain solve visual object recognition? *Neuron* **73**, 415–434 (2012).
- Tomita, H., Ohbayashi, M., Nakahara, K., Hasegawa, I. & Miyashita, Y. Top-down signal from prefrontal cortex in executive control of memory retrieval. *Nature* **401**, 699–703 (1999).
- Clopath, C., Busing, L., Vasilaki, E. & Gerstner, W. Connectivity reflects coding: a model of voltage-based STDP with homeostasis. *Nat. Neurosci.* **13**, 344–352 (2010).
- Graupner, M. & Brunel, N. Calcium-based plasticity model explains sensitivity of synaptic changes to spike pattern, rate, and dendritic location. *Proc. Natl. Acad. Sci. USA* **109**, 3991–3996 (2012).
- Pfister, J.P. & Gerstner, W. Triplets of spikes in a model of spike timing-dependent plasticity. *J. Neurosci.* **26**, 9673–9682 (2006).
- Shouval, H.Z., Bear, M.F. & Cooper, L.N. A unified model of NMDA receptor-dependent bidirectional synaptic plasticity. *Proc. Natl. Acad. Sci. USA* **99**, 10831–10836 (2002).

EDITORIAL SUMMARY

AOP: Experience-dependent synaptic modifications are one of the fundamental mechanisms of learning and memory, yet they are difficult to measure *in vivo*. Here the authors introduce a network model-based method that infers synaptic plasticity rules from the analysis of the statistics of neuronal responses to novel versus familiar stimuli.



ONLINE METHODS

Behavioral task and neurophysiology. For investigation of visual experience in inferior temporal cortex (ITC), we compared visual responses to novel and familiar stimuli measured in different sets of monkeys (*Macaca mulatta*) performing two different tasks (Figs. 1–4) in different laboratories. In a passive viewing task²², monkeys fixated stimuli that were presented for 200 ms with a 50-ms interval between stimuli. During the fixation, the responses of individual ITC neurons were measured with the stimulus sampled from 125 novel and 125 familiar images for each neuron. Activities of 73 putative excitatory neurons and 15 putative inhibitory neurons were recorded; cell types were classified from the width of their extracellularly recorded spikes⁵¹ (for more details, see ref. 22).

In another experiment²⁵, monkeys performed a dimming-detection task, which is similar to the passive viewing task except that monkeys were required to detect and indicate (by releasing a manual lever) a subtle decrease in luminance of the stimulus. The purpose of the dimming task was to require the animal to direct their attention to the stimulus. Ten familiar and eight novel images were presented during recordings for each neuron. Familiar images had been viewed many thousands of times over approximately 1 month of daily behavioral training sessions before recordings, and novel images had not been viewed before that session (but were repeated at least ten times per session). Each dimming-detection trial began when the animal grasped the manual lever, followed by the onset of a fixation spot. After acquiring gaze fixation (within a 2.0° radius window) for 500 ms, a single 100 × 100 pixel stimulus was presented foveally for a duration that was a sum of a fixed duration (650 ms) and a random duration (drawn from an exponential distribution with a mean of 200 ms). At the end of this duration, the image dimmed and the monkey was required to release the lever within 700 ms to receive a fruit juice reward. A total of 221 ITC cells were recorded from two monkeys, and, as in the passive viewing task, putative neuronal classes were determined from the spike widths. While the distribution of spike widths showed two peaks, they were not far enough apart to separate two populations clearly. Thus, to minimize potential misclassifications, we set well-separated thresholds of 500 μs and 250 μs for putative excitatory neurons and inhibitory neurons, respectively. With such thresholds, 41 and 27 neurons were classified as excitatory and inhibitory neurons, respectively.

The methods for neurophysiological recordings, surgery and behavioral task control for the second experiment have been described previously⁵². Briefly, neuronal recordings were conducted in both monkeys (male, 7–13 kg; research-naïve before these experiments) from ITC (areas TEa, TEm, TE2 and TE1; ref. 53), including the cortex on the lower bank of the superior temporal sulcus and the ventral surface of the ITC, lateral to the anterior medial temporal sulcus. The recording chambers were surgically placed stereotaxically, guided by magnetic resonance imaging scans conducted before surgery. Neuronal recordings were conducted with 1–4 tungsten microelectrodes (100 μm diameter) using multiple motorized microdrives (NAN Instruments) and multiple dura-piercing stainless steel guide tubes. All procedures were in accordance with the University of Chicago's Animal Care and Use Committee and US National Institutes of Health guidelines.

Data analysis in Figures 1–3. In both experiments, we obtained visual responses to each stimulus by taking the firing rate in the time window between 75 ms and 200 ms after stimulus onset. In Figures 2 and 4, showing input changes and learning rules in individual neurons, 125 visual responses to novel and familiar stimuli measured in a passive fixation task were used. In Figure 3, showing input changes from the distributions of firing rates averaged over many neurons, the number of visual responses was the product of the number of neurons and the number of stimuli (for example, 88 neurons × 125 visual responses in Fig. 3a). In the analysis of learning effects on input currents in individual neurons (Fig. 4), we showed input changes only in neurons having significantly different distributions for novel and familiar stimuli, which was determined by the Mann-Whitney *U* test at 5% significance level (30 excitatory neurons in Fig. 4a and 10 inhibitory neurons in Fig. 4b). In Figures 2g, 3 and 4a–d, noisy input changes were smoothed for presentation: after interpolating input changes at the equally spaced firing rates, we smoothed input currents locally using the lowess (locally weighted scatterplot smoothing) function with a span of 10% in Matlab. The significance of the input changes was computed by sampling multiple times from the same distribution of novel stimuli and computing the resulting input changes.

We show a 95% confidence level; that is, ± 1.96 times the s.d. of input changes at each postsynaptic firing rate.

Network model. To reproduce activity changes observed in the data, we considered a firing-rate model and a rate-based plasticity rule in the excitatory-to-excitatory connections. The network was composed of N_E excitatory and N_I inhibitory neurons. The firing rate of each neuron is denoted by r_i^l , with the superscript $l = E$ or I , and the subscript i represents the index of the neuron, ranging between 1 and N_l . These firing rates are governed by the equations

$$\begin{aligned}\tau_E \frac{dr_i^E}{dt} &= -r_i^E + \Phi_E \left(\sum_{j=1}^{N_E} W_{ij}^{EE} r_j^E - \sum_{j=1}^{N_I} W_{ij}^{EI} r_j^I + I_i^{EX} \right) \\ \tau_I \frac{dr_i^I}{dt} &= -r_i^I + \Phi_I \left(\sum_{j=1}^{N_E} W_{ij}^{IE} r_j^E + I_i^{IX} \right)\end{aligned}$$

where W_{ij}^{lm} is the strength of the synaptic connection from neuron j in population m to neuron i in population l with $l = E$ or I , $m = E$ or I , $i = 1$ to N_l , and $j = 1$ to N_m . Thus, excitatory neuron i receives recurrent inputs from excitatory and inhibitory populations and the external input I_i^{EX} , while inhibitory neurons receive recurrent excitatory inputs and the external input I_i^{IX} . The firing rate r_i^l approaches $\Phi_l(x_i^l)$ with intrinsic time constant τ_l , where $\Phi_l(x_i^l)$ represents the steady-state firing rate in response to total input current x_i^l .

We assumed that only the excitatory-to-excitatory connections are plastic and that the amount of the synaptic change depends on firing rates of pre- and postsynaptic neurons. We assumed that the dependence on pre- and postsynaptic terms is separable as $\Delta W_{ij}^{EE} = f_{\text{post}}(r_j^E) f_{\text{pre}}(r_i^E)$. Furthermore, we assumed that $f_{\text{pre}}(r_j^E) = r_j^E$, and, to prevent the mean weights after learning multiple stimuli from becoming too low, we added a constraint that the sum of synaptic weights over the presynaptic neurons is preserved with learning as

$$\begin{aligned}\Delta W_{ij}^{EE} &\leftarrow \Delta W_{ij}^{EE} - \frac{1}{N_E} \sum_{j=1}^{N_E} \Delta W_{ij}^{EE} \\ &= f_{\text{post}}(r_i^E) r_j^E - \frac{1}{N_E} \sum_{j=1}^{N_E} f_{\text{post}}(r_i^E) r_j^E \\ &= f_{\text{post}}(r_i^E) (r_j^E - \text{mean}(r^E))\end{aligned}$$

with W_{ij}^{EE} having lower bound 0 and upper bound w_{EE}^{max}/N_E . Note that this is equivalent to taking $f_{\text{pre}}(r_j^E) = r_j^E - \text{mean}(r^E)$. The remaining synaptic connectivity was assumed to be uniform; that is, $W_{ij}^{EI} = w_{EI}/N_I$ and $W_{ij}^{IE} = w_{IE}/N_E$ for all indices i and j .

In the simulation, $N_E = 4,000$, $N_I = 1,000$, $\tau_E = 20$ ms and $\tau_I = 10$ ms. $w_{EE}^{\text{max}} = 0.1$, $w_{EI} = 0.01$ and $w_{IE} = 0.5$, with the initial W_{ij}^{EE} set to be $w_{EE}^{\text{max}}/2N_E$.

The activity pattern for novel stimuli, the input current–output firing rate transfer function Φ , and the dependence of learning rules on postsynaptic firing rates $f_{\text{post}}(r_i^E)$ were obtained from the individual neuronal responses for novel and familiar stimuli averaged over neurons showing characteristic input changes; that is, excitatory neurons showing both depression and potentiation (green curves in Fig. 4a) and inhibitory neurons showing only depression (orange curves in Fig. 4b). In particular, $f_{\text{post}}(r_i^E)$ was derived from the dependence of input changes on postsynaptic firing rates Δh_i as

$$\begin{aligned}f_{\text{post}}(r_i) &\approx \frac{\left(\Delta h_i - \sum_{j=1}^{N_E} W_{ij}^{EE} \Delta r_j^E + \sum_{j=1}^{N_I} W_{ij}^{EI} \Delta r_j^I \right)}{\sum_j f_{\text{pre}}(r_j) r_j} \\ &\approx \frac{\Delta h_i - N_E m(W_{ij}^{EE}) (m(r^{E,\text{fam}}) - m(r^{E,\text{nov}})) + w_{EI} (m(r^{I,\text{fam}}) - m(r^{I,\text{nov}}))}{N_E \text{var}(r^{E,\text{nov}})}\end{aligned}$$

where $m(r^{l,\text{fam}})$ and $m(r^{l,\text{nov}})$ are average firing rates for familiar and novel stimuli of population $l = E$ or I , and $\text{var}(r^{E,\text{nov}})$ is the variance of the firing rates for novel stimuli, obtained from the data. $m(W_{ij}^{EE})$ is the average of excitatory to excitatory synaptic weights and is updated during initialization of the excitatory connections as the network learns multiple uncorrelated activity patterns. Because of the constraint on the sum of the synaptic weights, $N_E m(W_{ij}^{EE}) \approx w_{EE}^{\max} / 2$; that is, it remains close to its initial value.

Code availability. The data analysis and network simulations were performed in Matlab, and the code for network simulations are available upon request.

A **Supplementary Methods Checklist** is available.

51. McCormick, D.A., Connors, B.W., Lighthall, J.W. & Prince, D.A. Comparative electrophysiology of pyramidal and sparsely spiny stellate neurons of the neocortex. *J. Neurophysiol.* **54**, 782–806 (1985).
52. Ibos, G. & Freedman, D.J. Dynamic integration of task-relevant visual features in posterior parietal cortex. *Neuron* **83**, 1468–1480 (2014).
53. Paxinos, G., Huang, X.F. & Toga, A.W. *The Rhesus Monkey Brain in Stereotaxic Coordinates* (Academic, 2000).